Heliyon 8 (2022) e09724

Contents lists available at ScienceDirect

Heliyon

journal homepage: www.cell.com/heliyon

Research article

Synthesis and characterization of a heterogeneous catalyst from a mixture of waste animal teeth and bone for castor seed oil biodiesel production

Tamrat Getachew Mengistu [a], Ali Shemsedin Reshad [a,b,*]

[a] Department of Chemical Engineering, College of Biological and Chemical Engineering, Addis Ababa Science and Technology University, Addis Ababa, Ethiopia
[b] Center of Excellence for Sustainable Energy Research, Addis Ababa Science and Technology University, Addis Ababa, Ethiopia

ARTICLE INFO

Keywords:
Animal bone
Animal teeth
Calcination
Basicity
Castor seed oil biodiesel
Characterization

ABSTRACT

The present study focused on the synthesis of heterogeneous catalyst from a mixture of waste animal teeth and bone through thermal method. The produced catalyst was used for castor seed oil (CO) biodiesel production. A different mixing ratio of teeth and bone was used with a calcination temperature range from 650 °C to 1250 °C with 100 °C increment for 3h calcination duration. Thermogravimetric analysis (TGA) for animal teeth and bone was performed to identify the common decomposition temperature range. The effect of calcination temperature on basicity of the catalyst and yield of biodiesel was studied for each teeth and bone mixing ratio. Maximum basicity of 6.12mmol HCl/g and biodiesel of 89.5wt% was obtained by mixing ratio of 25wt% teeth and 75wt% bone at calcination temperature of 1150 °C for 3h. The purity of the produced biodiesel in terms of mono fatty acid methyl esters (FAME) formation was found to be 92.6%. X-ray Diffraction (XRD), X-Ray fluorescence (XRF), Fourier-transform infrared spectroscopy (FT-IR) and TGA was used to characterize the raw and produced catalyst. The maximum yield of FAME (89.5wt% with 92.6% purity) was obtained by 5wt% catalyst loading and 9:1 M ratio of methanol to castor seed oil at 60 °C reaction temperature for 3h. Compositional analysis of the produced CO FAME was performed by FT-IR, gas chromatography-mass spectroscopy (GC-MS) and nuclear magnetic resonance (NMR). The performance of the produced catalyst was also checked using its reusability for trans-esterification CO. Further, the physico-chemical properties including rheological properties of the produced CO FAME were characterized by ASTM methods to check its suitability as a liquid biofuel.

1. Introduction

Biodiesel is a long-chain fatty acid of mono alkyl ester and obtained from triglycerides of animal fat, edible and non-edible vegetable oil. It is an alternative fuel to petroleum diesel fuel and biodegradable, non-toxic and emits lesser amount of net carbon dioxide (CO_2) than petroleum diesel fuel to the environment [1,2,3]. Vegetable oils are usually esters of glycerol with different chain lengths of fatty acid alkyl groups and degrees of saturation and unsaturation. It may be seen that biodiesel derived from vegetable oil contains a substantial amount of oxygen molecules which contribute to complete combustion in engine [4]. Castor seed oil, soybean oil, sunflower oil, jatropha seed oil, cotton seed oil, palm seed oil are the most common feedstocks for biodiesel production [5]. Castor seed oil is a viscous, pale yellow, non-volatile, non-drying oil with a bland taste, sometimes used as a purgative, non-edible and obtain from castor seed through chemical and mechanical extraction [6]. The high viscosity and water content properties of castor seed oil make it difficult to use as a fuel. Transesterification is the most common and simpler chemical modification for vegetable oil as to use as fuel diesel engine (Figure 1) and upgrading methods of vegetable oil which improves important oil fuel properties [7]. The most common alcohols used for transesterification reactions are methanol, ethanol propanol and butanol [1].

Different catalysts are used to increase the rate of transesterification reaction which are either homogenous, heterogeneous or biocatalyst (Figure 1) [3]. Homogeneous catalysts are more sensitive for higher free fatty acid (FFA), moisture content and difficult to recovery the catalyst after reaction completed. Further, the homogeneous catalyst used for the reaction increases waste water generation during purification steps. Enzymatic catalysts are more expensive due to catalyst preparation cost and also catalysts are inhibited by alcohol whereas heterogeneous catalysts are the cheapest catalyst due to the ability of recyclability and product purity [8,9]. Alkali heterogeneous catalysts are very fast as compare to acid heterogeneous catalysts and slower than homogeneous

* Corresponding author.
E-mail address: ali.shemsedin@aastu.edu.et (A.S. Reshad).

https://doi.org/10.1016/j.heliyon.2022.e09724
Received 9 February 2022; Received in revised form 2 May 2022; Accepted 9 June 2022

alkali catalyst [10]. The most common heterogeneous alkali catalysts are calcium oxide (CaO), magnesium oxide (MgO) and barium oxide (BaO). One of the problem that faced in biodiesel production is the cost of production such as catalyst, purification and feedstock cost that makes the biodiesel not competitive and fail to produce on large scale [11]. Hence, utilization of an alternative types of catalysts derived from waste materials is one way to reduce the cost of production. Waste animal bone and teeth have a potential to use as source of heterogeneous catalyst which may reduce the production cost of biodiesel. The most common abattoir solid waste is animal bone where one cattle contribute 30.4% of bone waste from its total waste of the cattle [12]. Around 0.13 billion tones of waste animal bones are generated per year by the meat producer industry in the world to meet the meat consumption of the population [13]. On the other hand, waste animal bone and teeth obtained from abattoir pollute the environment by favoring the reproduction system of pathogenic microorganisms by exerting oxygen [14]. Both animal teeth and bone are possessed hydroxy apatite chemical which has full of calcium and phosphorus inorganic minerals with good thermal stability and porous crystal structure that helps transesterification reaction through the surface-active site [15,16,17,18].

Obadiah et al. [16] used calcined animal bone as a source of heterogeneous catalyst which was obtained at 800 °C calcination temperature for transesterification of palm oil for FAME production. About 96.78wt% yield of FAME was obtained at 65 °C, 20:1, 20wt% and 4h reaction temperature, methanol to oil molar ratio, catalyst loading and reaction time, respectively. Smith et al. [18] reported 97wt% yield of soybean oil base FAME obtained through reaction temperature 65 °C, reaction time 3h with methanol to oil ratio of 6:1 using calcined animal bone. Further, waste animal bone was used for jatropha oil base FAME production through the calcination of the bone at 900 °C with transesterification reaction parameters of 70 °C reaction temperature, 3h reaction time with 9:1 methanol to oil molar ratio to obtain 96.1wt% yield of FAME [19]. Ostrich bone calcined at 900 °C was also used to obtain 90.56wt% yield of FAME from waste cooking oil with 60 °C reaction temperature, 15:1 methanol to oil molar ratio, 4h reaction time and 5wt % catalyst loading [20]. Calcined animal, fish and chicken bone was used as a catalyst to obtain greater than 93wt% yield of FAME [21,22,23]. It was also found in the literature that many studies were conducted on vegetable oil transesterification reaction using either animal, chicken or fish bone as catalyst. There may be an issue of raw materials scarcity for mass scale production of heterogeneous catalyst for transesterification reaction from single raw material like animal bone. Thus, utilizing of various parts of animal wastes is promising option to overcome the challenge of raw materials scarcity for catalyst synthesis for mass scale production. To the best of our knowledge, mixture of waste animal teeth and bone was rarely studied for heterogeneous catalyst for transesterification reaction to produce castor seed oil biodiesel. Hence, the present study was aimed to synthesis heterogeneous catalyst from mixture of waste animal teeth and bone. The catalyst was used for FAME (biodiesel) production. Further, the rheological behaviours of castor seed oil biodiesel produced through mixture of waste animal teeth and bone catalyzed transesterification process were also investigated.

2. Materials and methods

2.1. Materials

Waste animal bone and teeth were collected from Abattoirs slaughter in Fiche town around Oromia region; Ethiopia. Castor seed oil (Table 1), methanol (94%) and ethanol (95%) were purchased from loba Chemie. pvt. Ltd, Mumbai, India. Sulfuric acid (98%), phenolphthalein (99.9%), Iodine monochloride, glacial acetic acid (99.5), Potassium hydroxide, sodium hydroxide, Sodium thiosulfate solution, Chloroform and Hydrochloric (95%) were the product of Himedia Laboratories Pvt Ltd and Sisco Research Laboratories Pvt. Ltd.

2.2. Catalyst synthesis

2.2.1. Sample preparation

The collected waste animal bone and teeth were shaved by using knife to remove sticking organic parts like meet and cartilage and then boiled by using de-ionized water for several times until white bone and teeth were observed by necked eye. Then the washed waste animal bone and teeth were sun dried for 72h and followed by oven–dried for 48 h at 120 ± 5 °C. The dried samples (i.e. animal bone and teeth) were crushed individually by jaw crusher followed milled by mortar and pestle to obtain in powder form with particle size range below 250μm.

2.2.2. Calcination of animal bone and teeth

Thermogravimetric analysis (TGA) of powder bone and teeth were analyzed to identify the calcination temperature range. The powder bone and teeth samples are mixed with different mixing ratios of 0:100, 25:75, 50:50 and 100:0 by weight. About ten gram of the mixtures were placed in ceramic crucibles and calcined by muffle furnace (MV106 model, USA) for 3h at different calcination temperature from 650 °C to 1250 °C with an increment of 100 °C. After calcination process the synthesized catalyst was placed in desiccator till to cool and then used for further process.

2.3. Catalyst characterization

2.3.1. XRD and XRF analysis

Crystal structure of the raw and produced catalyst were determined by X-ray Diffraction (XRD-7000 model) with the Cu Kα radiation using an acceleration voltage of 40 kV, current of 30 mA, over a 2θ range of 5–85° at a scanning speed of 3°/min and continues scanning mode were used to record the XRD patterns of the catalyst and finally the peak associated were analyzed. The crystallinity index of the sample was estimated using Eq. (1) [24]. Further, XRF (X-Ray Fluorescence) was used for compositional analysis of the raw sample and catalyst in the form of oxides.

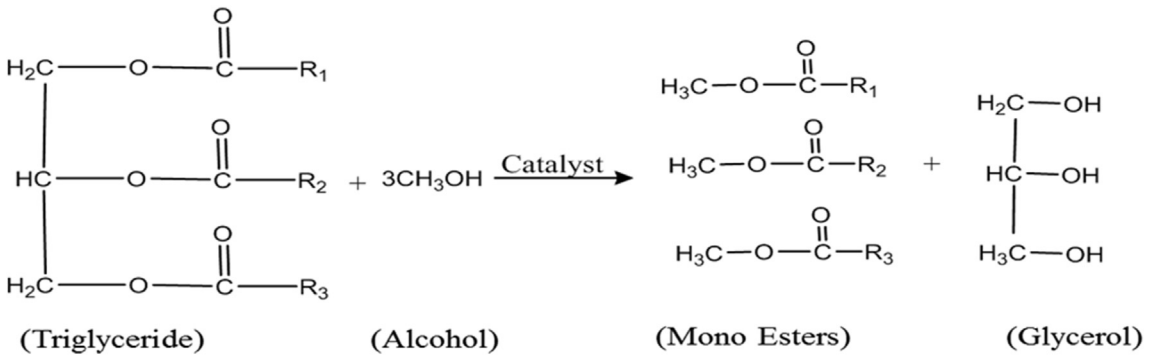

Figure 1. Overall transesterification reaction for any triglycerides with fatty acid alkyl groups of R_1, R_2 and R_3.

$$Xc = \frac{I300 - V112/300}{I300} \times 100 \quad (1)$$

Where: X_c is a fraction of crystallites, I_{300} intensity at 3,0,0 induces and $V_{112/300}$ is the intensity of the trough between (112) and (300) diffraction peaks of Hap.

2.3.2. FT-IR analysis

Fourier transform infrared (FT-IR) spectroscopy was used to analyze the functional groups present in raw animal bone, raw animal teeth and calcined animal bone and teeth. The grounded sample was exposed to the beam of infrared light through iS50 ABX model. The spectra were obtained at a resolution of 4cm^{-1} in the wave number range of 4000cm^{-1} to 400cm^{-1}.

2.3.3. Thermal decomposition

Animal bone and teeth powder common decomposition temperature range and thermal properties of the produced catalyst were analyzed using thermogravimetric (TG) method (HTC–1 model). The TG was operated at a heating rate of 10 °C/min under nitrogen atmosphere (0.01L/min). Sample amount of 20mg was place in the sample holder. Then the sample was heated from 30°C–1000 °C under a nitrogen atmosphere with a flow rate of 0.01L/min and online measurement of the weight loss versus temperature and/or time was recorded using inbuilt software.

2.3.4. Basicity

Basicity of catalyst is the amount of basic sites on a solid per unit weight of solid sample usually expressed as the numbers of mmol of basic sites per unit weight of the solid [25,26]. The basic strength of the solid catalyst surface is defined as the ability of the surface to convert an adsorbed electrically neutral acid to its conjugate [26,27]. The basicity of the raw samples and the prepared catalyst were measured using titration method [27,28]. About 0.2g of sample was added in 50ml of 0.2N HCl solution and mixed until the sample completely dissolved. Then three drops of phenolphthalein indicator were added in the solution. Finally the solution was titrated with 0.2N of KOH solution till color change observed then the basicity was estimated by Eq. (2).

$$B_c = \frac{0.2 \times (V_{HCl} - V_{KOH})}{M_s} \quad (2)$$

Where: B_c is basicity (mmol HCL/g of sample), V_{HCl} is amount of 0.2N of HCl used for titration, V_{KOH} is amount of 0.2N of KOH required to titrate the HCl acid and M_s is mass of the sample in gram.

2.4. Transesterification reaction

Transesterification reaction was used to test the performance of the synthesized catalyst. The reactions were performed in 500ml three-neck round bottom flask with a hot plated magnetic stirrer and fitted condenser with cool water to reduce evaporation of methanol. The reaction condition such as reaction time (3h), molar ratio (9:1), catalyst loading (5wt%), reaction temperature (60 °C) and string speed (1500rpm) was set based of the different reaction conditions reported on the literatures [18,19,21,28]. Known amount of oil sample with 9:1 M ratio of methanol to oil was prepared and heated to 105 °C for 25 minute to remove unbounded moisture if any and cooled to reaction temperature (60 °C). On the other separate flask known amount of methanol and catalyst (5wt%) samples were mixed in the flask and an exothermic nature was observed which confirms the formation of methoxides. Then the methoxides and the cooled oil sample were added to the glass reactor for reaction. The reaction was take place at 60 °C temperature for 3h at 1500rpm string speed. After the reaction completed, the reaction mixture was put in centrifuge (pro-Analytical C2004 model) at 3000rpm for 30 minute to separate catalyst then the rest solution was put in a 500ml separating funnel for overnight. The glycerol part at bottom was removed and the top layer which was mixture of biodiesel and methanol were washed for four times with warm water. Then sample placed into rotary evaporator to remove the remaining methanol and water. The amount of the obtained biodiesel was weighed and the yield of biodiesel with respect to the amount of castor seed oil used during the reaction was estimated by Eq. (3) [29,30,31,32,33]. Further, the purity of the obtained biodiesel in terms of mono FAME formation was determined using ^{1}H NMR analysis (eq. 4) [34,35].

Table 1. Physico–chemical properties of castor oil.

Properties	Unit	Value
Specific gravity at 20 °C	g/cm^3	0.957–0.961
Acid value	mg of KOH/g	0.562
Saponification value	mg of KOH/g	177.43
Iodine value	gI_2/100g	85
pH	–	6.52
Refractive index	–	1.456–1.515
Hydroxy value	–	160–168

$$Yield\ (wt\%) = \frac{\text{Weight of produced biodiesel}}{\text{Weight of castor seed oil used}} \times 100 \quad (3)$$

2.5. Characterization of castor seed oil fatty acid methyl esters (biodiesel)

Physico-chemical properties such as density, viscosity, acid value, free fatty acid, saponification value, calorific value, cetane number and iodine value the samples were estimated/determined as per American Society for Testing and Materials (ASTM) methods [36,37].

Further, the conversion (purity of produced biodiesel) of the triglycerides of castor seed oil was monitored quantitatively and qualitatively using nuclear magnetic resonance (^{1}H NMR and ^{13}C NMR). About 60μl biodiesel sample was taken in a 5mm NMR tube and mixed with 500μl deuterated chloroform ($CdCl_3$) solvent. The chemical shift peak of deuterated chloroform at 7.26ppm, methyl ester proton at around 3.65ppm and methylene proton at around 2.31ppm were taken from ^{1}H NMR and used for conversion (purity of produced biodiesel) estimation [34]. The following equation (eq. 4) was used to determine the conversion (X) of triglycerides of castor seed oil into its mono fatty acid methyl esters:

$$X(\%) = \frac{2 \times A_{ME}}{3 \times A_{\alpha-CH_2}} \times 100 \quad (4)$$

Where; X (%) is percentage conversion of castor seed oil (CO) triglycerides, A_{ME} is integration value of methyl ester proton peak area at around 3.65ppm in ^{1}H NMR profile and $A_{\alpha\text{-}CH2}$ is integration value of carbonyl methylene proton peak area at around 2.31ppm.

Additionally, the castor seed oil biodiesel sample was analyzed by gas chromatograph-mass spectrometer (GC-MS) (GC-MS OP 5000 series, Shimadzu Japan, 2010) to identify the fatty acid composition. Capillary column of 60m length, 0.25mm internal diameter and 0.25μm thickness was used for the separation of esters. Three minutes of equilibrate time was set to rise the temperature to 150 °C and maintained isothermal temperature for 5 minutes, then raised to 250 °C at the rate of 7 minutes and final temperature maintained for 10 minutes. An ionization voltage of 70Ev over the very scanning range of 450–750amu was used to fragment the components. The components of the samples were identified by comparing the mass spectra with national institute of standards and technology research library (NIST-2014). Other operating conditions

were injector temperature of 250 °C, interface temperature of 240 °C and ion source temperature of 200 °C.

2.6. Rheological behaviour of castor seed oil biodiesel

The rheological properties of produced castor seed oil biodiesel were carried out on Anton Paar MCR–102 Rheometer using SCS geometry (Solid Cylindrical shape Fixture). Sample volume of 50ml and a heating rate of 1 °C/min from 10 °C to 80 °C under constant mechanical shear rate range from $50s^{-1}$to $300s^{-1}$ were considered for rheological properties test. A rotational type test was used with a 3mm gap and the cooling water unit was used to maintain temperature. Finally, the viscosity versus shear stress profile was analyzed by power law model.

3. Results and Discussion

3.1. Characterization of animal bone and teeth before calcination

Before the catalyst was synthesized; the ground waste animal bone and teeth were characterized by TGA and FT–IR to identify the common decomposition temperature and the functional group present in the sample, respectively.

The thermal decomposition of animal bone and teeth are presented in Figure 2. It can be observed that, the thermal decomposition of both the sample were takes place in two stages. The first stage (30–200 °C) was attributed to removal of unbounded water molecules and biological parts such as tissues in uncalcined animal teeth and fragmentation of macromolecules such as collagen and proteins decomposition in uncalcined animal bone [19,38]. The second stage was observed from 200–650 °C and 200–550 °C for animal teeth and animal bone, respectively. The second stage decomposition in both samples may be due to the further removal of collagen and mucopolysacharide gel and decomposition of $CaCO_3$ to CaO [38,39]. Moreover, the evolution of gaseous element was resulting in the formation of hydroxyapatite [28]. The weight loss beyond 650 °C for teeth sample and 550 °C for bone sample is very small which is attributed to carbonate apatite decomposition and the formation of gaseous elements which further led to the formation of inorganic residue consisting of hydroxyapatite and complete decomposition [19, 23,40]. The DTG result shows that the maximum decomposition was obtained at 360 °C with rate of 0.084wt%/min and 400 °C with 0.026wt %/min for animal bone and teeth, respectively. Additionally, the DTG result also shows that higher rate of decomposition was observed for animal bone with lesser temperature as compared to animal teeth. A total of 25wt% and 16wt% mass loss was obtained for animal bone and teeth with thermal decomposition temperature range from 30 to 550 °C and 30–650 °C for animal bone and teeth samples, respectively. Similar result was reported for pig bone and teeth [41]. Hence, temperature of 650 °C was used as lower temperature for calcination of during catalyst preparation.

The functional group vibration occurred due to incoming infrared light created dipole moments of vibration occurred in FT-IR [42]. The FT–IR spectra of the vibrational origin of the phosphate, carbonate, amide groups and other inorganic components are shown in Figure 3. The C–O asymmetric stretching and bending modes were observed at a wavenumber of $1410cm^{-1}$, $1412cm^{-1}$ and $870cm^{-1}$, $872cm^{-1}$ for bone and teeth samples, respectively. This result indicate that the presence of highly crystalline calcium carbonate in the form of hydroxyapatite [18, 43]. Spectra at wave number $1015cm^{-1}$ and $1019cm^{-1}$ corresponded to asymmetric P–O bond stretching for bone and teeth, respectively [44]. O–P–O bond vibrations were observed at wave numbers of $558cm^{-1}$ and $561cm^{-1}$ [20,44,45]. This indicated the presence of phosphate group in the form of PO4-3. Bending and stretching vibrations OH^- group mode was observed at $1640–1642cm^{-1}$ and 3580 cm^{-1} [45,46]. The raw bone and teeth peak was very broad and blended with organic substances, but the stretching frequencies of derived HAp were crisp and unambiguous. Other absorption peaks were discovered in raw bone and teeth at

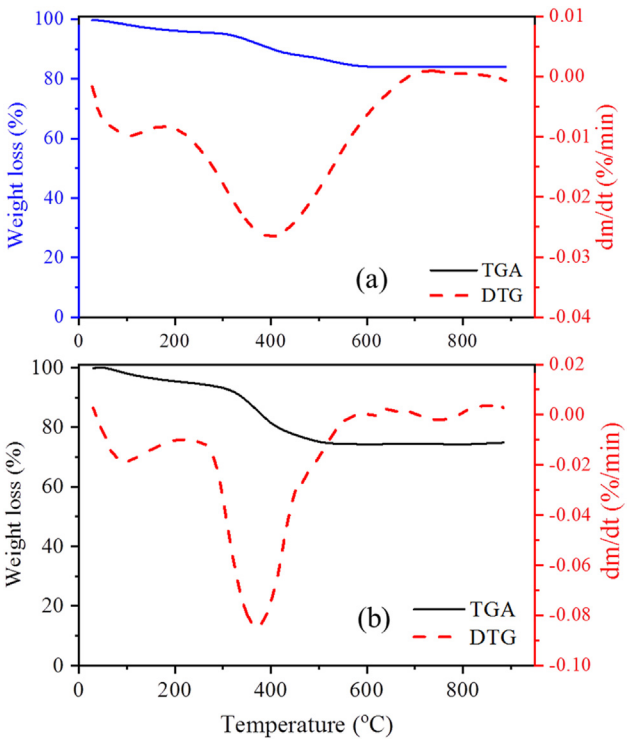

Figure 2. TG and DTG analysis uncalcined samples for (a) waste animal teeth and (b) waste animal bone.

$2922cm^{-1}$ and $1640–1642cm^{-1}$, which correlate to N–H stretching and amide bonds, indicating the existence of biological materials like protein [47]. Where a similar investigation was also reported for uncalcined animal bone [28], Thunnus obesus bone [47] and bovine teeth [48].

3.2. Calcination temperature and basicity

The relationship between calcination temperature, mixing ratio of animal bone and teeth and basicity of produced catalysts are shown in Figure 4. Based of the basicity of the catalyst results, the values were initial increase for all mixing ratio between 650 °C and 950 °C calcination temperature as compered to calcination temperature beyond 950 °C. The catalyst obtained from 100wt% animal bone found to be a higher basicity as compared to the other mixing ratio within calcination temperature range of 650 °C–950 °C. The results presented in Figure 4 indicate that an increased basicity value due to formation of calcium oxide (higher basic strength) as the calcination temperature increased [49]. The value of basicity reaching maximum of 6.07mmol/HCl at 950 °C and reduced the basicity from 6.07–5.89mmol/HCl as the calcination temperature rose above 950 °C for animal bone. A higher temperature may resulted in the suppression of basicity of the catalyst due to the high sintering rate of the catalyst [19]. Over the calcination temperature range of 650–950 °C, the basicity of the 100wt% calcined teeth was lower, but the basicity increment value for each 100 °C calcination temperature increment was substantially higher than that of the other mixing ratio of the catalysts (Figure 4). As the calcination temperature increased from 650 °C to 950 °C which enhanced the total basicity of the catalyst obtained from mixture of 25wt% teeth and 75wt% bone from 2.65 to 6.0mmol HCl/gram and attain a slightly higher basicity value of 6.12mmol HCl/g at the calcination temperature of 1150 °C. However, above the calcination temperature of 950 °C the proximity similar basicity value for each mixing ratio of the catalysts were observed (Figure 4). In a similar study on fishbone calcined at a temperature of 900 °C depicted 16.3mmol HCl/gram of basicity [22]. Calcined Ostrich bone at the temperature of 900 °C reported a basicity of 13.3mmol HCl/g [20].

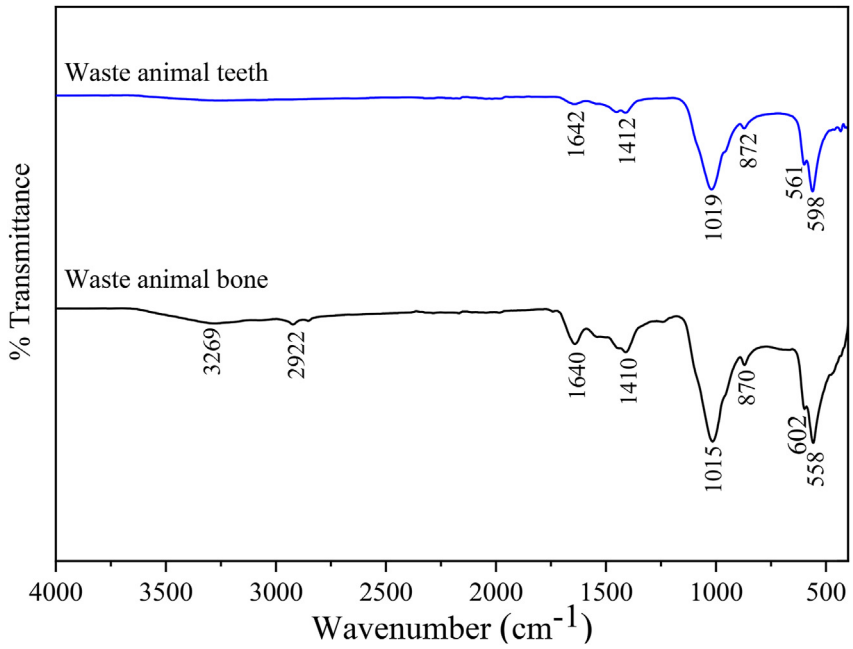

Figure 3. FT-IR spectra of uncalcined waste animal teeth and bone.

3.3. Performance of the synthesized catalyst on fatty acid methyl ester production

The catalytic performance of each mixing ratio of synthesized catalyst obtained at different calcination temperatures were tested on the transesterification reaction (Figure 1) for castor seed oil (CO) and the obtained results are presented in Fig. 5a–e. As can be seen from the result the basicity of the catalyst shows great influence on catalyst performance to maximize the yield of fatty acid methyl ester (Fig. 5a–e). The catalytic performance of calcined teeth (100wt%) catalyst with 2.65–5.85mmol HCl/g on the transesterification of castor seed oil was found to be 60.3–83.89% yield of castor seed oil fatty acid methyl ester (Figure 5a). The result was lower as compared to other mixing ratio and 100wt% pure bone catalyst (Fig. 5b–e). The obtained result indicated that the basicity of the catalyst has a positive influence on the yield of castor seed oil biodiesel. Similar finding was reported for soybean oil biodiesel production using metal oxide heterogeneous catalyst [27]. Furthermore, Figure 4 shows that calcination temperature beyond 950 °C has no significant effect on basicity of the calcined catalyst.

The effect of calcination temperature on the yield of castor seed oil biodiesel during transesterification reaction using the mixture of animal teeth and bone source catalyst is shown in Figure 6. As shown in Figure 6,

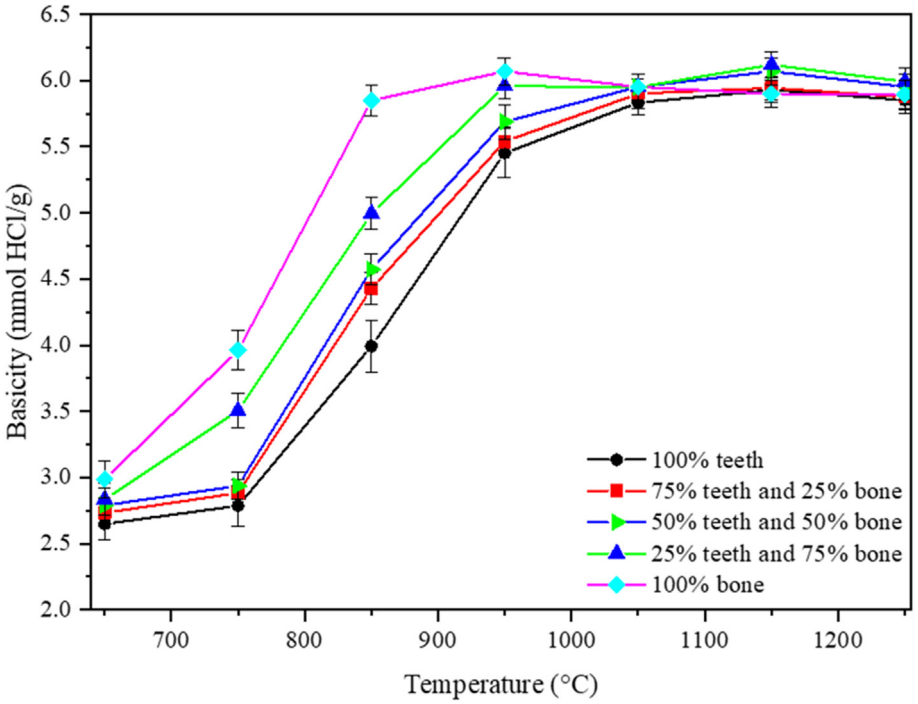

Figure 4. Effect of calcination temperature on basicity of the produced catalysts for various mixing ratio of waste animal teeth and bone.

the biodiesel yield for the catalyst obtained from animal bone is higher than that of teeth source catalyst below 950 °C calcination temperature. However, the yield of biodiesel was proximity similar beyond 950 °C calcination temperature and the values were decreased.

To observe the effect of the calcination temperature on the catalyst activity, both animal teeth and bone were mixed at various weight ratios and calcined at different temperature ranging from 650 to1150 °C and increased the yield of biodiesel (Figure 6). This result is attributed to desorption of carbon dioxide from animal teeth and bone at higher calcinations temperatures which producing basic sites that catalyzed the transesterification reaction [16]. However, calcination beyond 1150 °C reduced the yield of castor seed oil biodiesel. This could be due to the catalyst particle agglomeration and sintering of the fine particles of the sample at higher calcination temperature [16,19,35].

For a mixture of 25wt% animal teeth and 75wt% animal bone as calcination temperature increased above 950 °C approaches higher basicity and yield of castor seed oil biodiesel and loss it catalytic activity as the calcination temperature increased beyond 1150 °C. This result maybe due to the existence of micropores and low pore volume on the surface of the catalyst which reduces the catalytic performance [18]. Maximum of 89.5wt% yield of CO FAME was obtained at 1150 °C synthesized catalyst of 25wt% teeth and 75wt% bone mixture catalyst with higher basicity value of 6.12mmol HCl/gram of catalyst (Figure 5d). Similarly, the previously investigation on catalyst obtained from a calcined fishbone, calcined ostrich bone and K_2CO_3 supported CaO basicity was 16.23, 13.3 and 0.96mmol HCl/g and achieved 97.73, 90.56 and 93% yield of biodiesel, respectively [20,22,50]. Further, the catalytic performance of the produced catalyst was comparable with the reported yield of biodiesel (Table 2) [16,18,19,20,21,22,23,28]. For example, proximity similar yield of CO biodiesel (89.5wt%) was obtained with lesser catalyst loading (5wt%) using the produced catalyst as compared to 18wt% cow bone for soybean oil biodiesel [21] and 10wt% MFAAB for mustard oil biodiesel [28]. Additionally, catalyst produced from mixture of animal teeth (25wt %) and bones (75wt%) was tested for its reusability for transesterification of CO triglycerides (Table 3). The reusability of catalyst was investigated using similar reaction parameters. The catalyst performance was reduced by 12% from 89.5wt% to 78.04wt% used after four times and to 72.0wt% after fifth recycle. Similarly, calcined animal bone and chicken bone were reused a four time with comparable catalytic properties with fresh catalyst [16,19,23]. Furthermore, the experimental results showed that mixing ratio of 25:75 of animal teeth to bone on weight bases and calcination temperature of 1150 °C for 3h is considered to be the most appropriate condition for utilization of both waste animal teeth and bone as raw materials heterogeneous catalyst synthesis through calcination method for castor seed oil biodiesel production.

3.4. Characterization of the synthesized catalyst

The mixing ratio of the catalyst 25wt% animal teeth and 75wt% animal bone with 1150 °C calcination temperature was higher basicity and yield of CO FAME was further characterized using several techniques. The FT-IR spectra of calcined catalyst obtained from mixture of 25wt% animal teeth and 75wt% animal bone is presented in Figure 7. From the FT–IR analysis, the peak at 3272 cm^{-1} indicates a hydrogen bond which

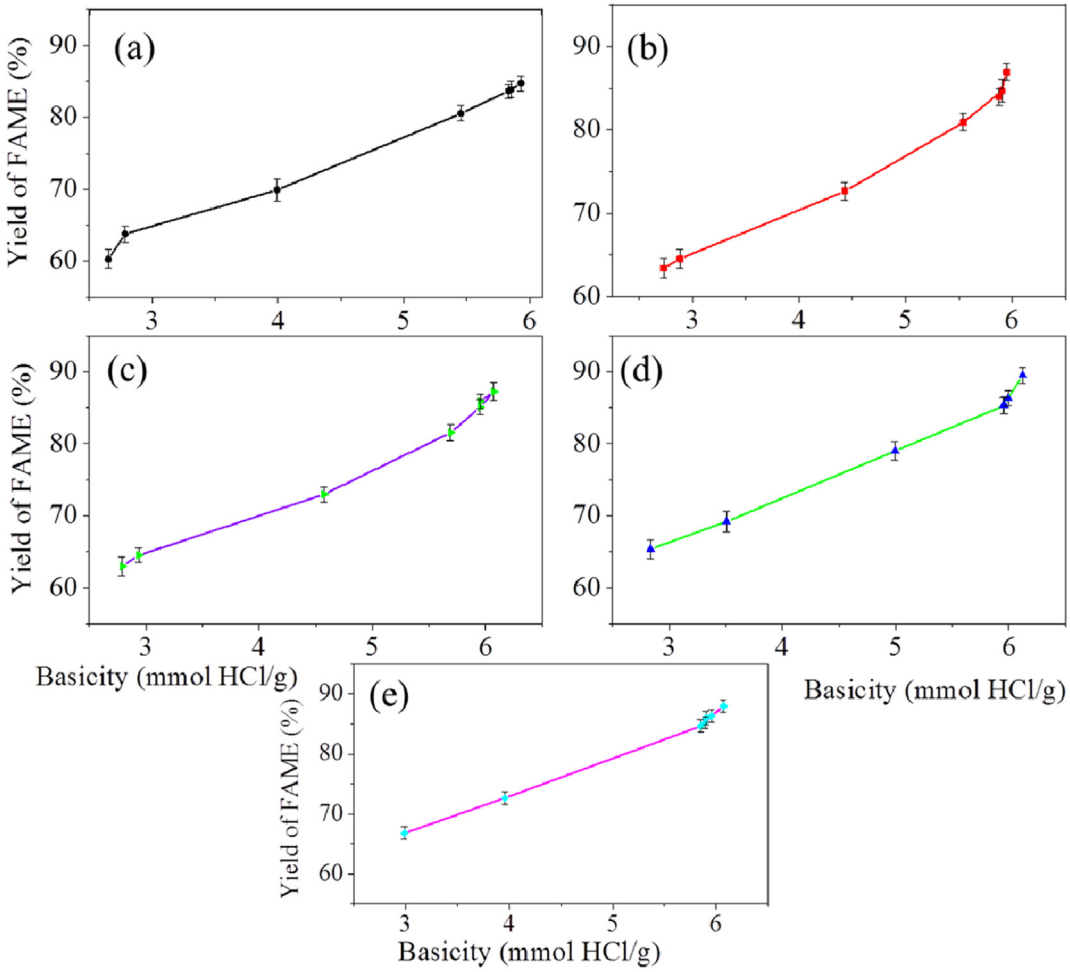

Figure 5. Effect of basicity of the produced catalysts on the yield of FAME for various mixing ratio of waste animal teeth and bon: (a) 100% teeth, (b) 25% bone and 75% teeth, (c) 50% teeth and 50% bone, (d) 25% teeth and 75% bone and (e) 100% bone.

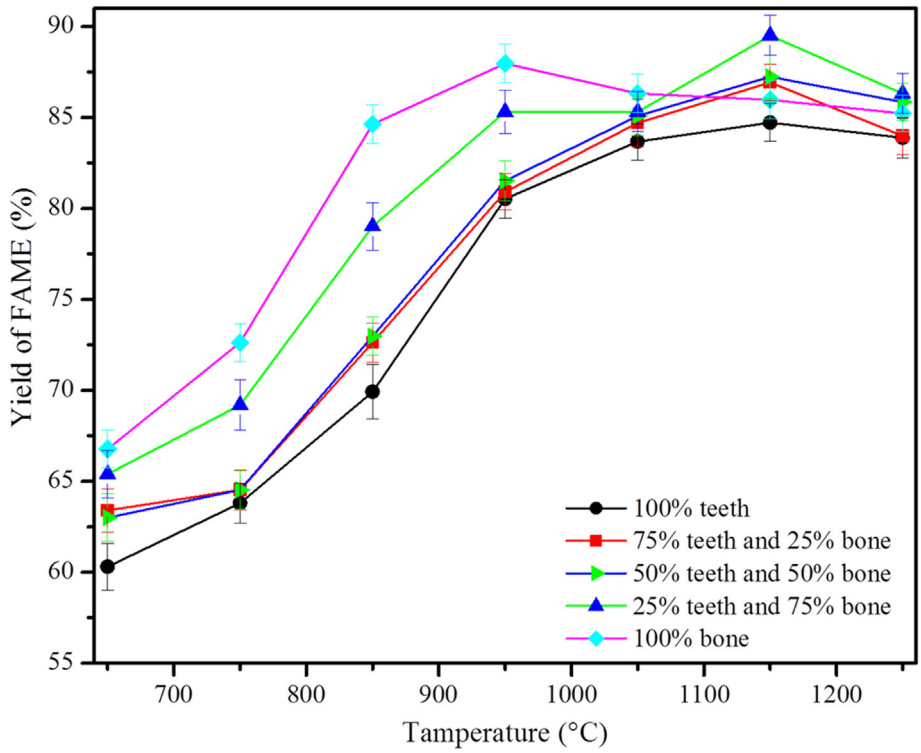

Figure 6. Effect of calcination temperatures on the yield of castor seed oil fatty acid methyl ester for various mixing ratio.

confirms the existence of hydrate (H_2O) or hydroxyl (-OH). The small peak was observed for uncalcined mixture of 25wt% animal teeth and 75wt% animal bone at 2922cm^{-1} and 2500–2000cm^{-1} which indicated the presence of organic part in the form of protein, a single bond of N–H, C–H and triple bond of carbon with carbon and nitrogen that are not found in the thermally treated bone [41,47]. The existence of CO^{-2}, PO_4^{-3} and PO_4^{-3} were observed at 1458, 1032 and 566cm^{-1}, respectively whereas after calcination all water and organic indicator functional groups was absent in the calcined sample (Figure 7). The results were supported by the TGA of the sample before (Figure 2) and after calcination (Figure 8) and an additional peak was also observed for calcined mixture at 630cm^{-1} which indicated the appearance of OH^{-1} [20,41]. At the peak of 1411cm^{-1} in the uncalcined mixture, carbonate groups are united with the organic part, whereas peaks 1458cm^{-1} in the calcined catalyst revealed carbonate groups free of organic matter. This demonstrates that the organic part was removed and that carbonated HAp crystals were formed.

Table 3. Reusability of the catalyst for CO transesterification reaction obtained from 25wt% animal teeth and 75wt% animal bone and calcined at 1150 °C.

Recycling	CO FAME yield (wt%)
Fresh catalyst	89.5
Frist recycle	87.56
Second recycle	85.32
Third recycle	82.02
Fourth recycle	78.04
Fifth recycle	72.00

Figure 8 shows that following calcination only 0.5–1wt% weight loss was observed with the temperature range of 25–900 °C. The results indicate that the synthesized catalyst was thermally stable and the thermal decomposition of mixture of animal teeth and bone completed

Table 2. A comparison of heterogeneous catalyst performance for biodiesel production various feed stocks.

Catalyst synthesis conditions			Transesterification reaction conditions					Yield (%)	Reference
Catalyst source	Calcination		Oil source	Molar ratio	Catalyst loading (wt %)	Reaction			
	Temperature (°C)	Time (h)				Temperature (°C)	Time (h)		
[a]MWATB	1150	3	Castor	9:1	5	60	3	89.5	Present study
Animal bone	800	–	Palm	6:1	20	65	4	96.78	Obadiah et al., 2012 [16]
Bovine bone	750	6	Soybean	6:1	8	65	3	97	Smith et al., 2013 [18]
Animal bone	900	–	Jatropha	9:1	6	70	3	90.1	Nisar et al., 2017 [19]
Ostrich bones	900	4	[c]WCO	15:1	5	60	4	90.56	Khan et al., 2020 [20]
Cow bone	800	4	Soybean	10:1	18	60	3	92.2	Ayoola et al., 2018
[b]MFAAB	900	2	Mustard	5.5:1	10	65	6	90.4	Volli et al., 2019 [28]
Fish bone	~1000	2	Soybean	6.27:1	1.01	60	5	97.73	Chakraborty et al., 2011 [22]
Chicken bone	900	4	[c]WCO	15:1	5	65	4	89.93	Farooq et al., 2015 [23]

[a] MWATB: Mixture of waste animal teeth and bone.
[b] *MFAAB:* Mixture of fly ash and animal bone.
[c] WCO; Waste cooking oil.

up on calcination. The minor weight loss in the temperature range of 25–900 °C indicated the synthesis of gaseous elements, which eventually led to the formation of inorganic residue, which is hydroxyapatite and calcium oxide and absorption of atmospheric moisture by the sample [20]. But before calcination the mixture of 25wt% teeth and 75wt% bone about 7% weight loss was observed with the temperature range from 25–300 °C and additional 20.55wt% mass loss was also observed from 300–590 °C. The weight loss attributed to the presence of moisture, protein and some other fatty matter which was volatilized and decomposed upon calcination (Figure 8).

The XRD pattern for uncalcined and calcined catalyst of a mixture of 25wt% teeth and 75wt% bone are shown in Figure 9. The result confirms the existence $CaCO_3$ in two separate phases of aragonite and calcite in the form of hydroxyapatite peak at 2θ of 28.48°, 39.93°, 42.39°, 49.4° and 26°, 31.85°, 32.82°, 34.5°, 42.39°, 47.03°, 51.37°, respectively (Figure 9) [19]. The calcination process accelerates the breakdown of calcium carbonate into calcium oxide and calcium hydroxide, which was present in the uncalcined mixture of teeth and bone [24]. From Figure 9 for calcined mixture of teeth and bone, the peaks at 2θ of 10.86°, 21.78°, 25.88°, 32.92°, 39.82°, 46.72°, 46.32°, 51.43°, 57.61°, 60.42°, 62.94° and 65.12° are attributed to the presence of hydroxyapatite [20,22,23] and all the peaks values of the 2θ were comparable with Joint Committee on Powder Diffraction Standards (JCPDS–09–0432). The peaks at 2θ of 28.15°, 29.17° and 31.81° are an indicator of β–Ca_3 $(PO_4)_2$ phase that produced from hydroxyapatite that act as a base catalyst for transesterification reaction [51]. The peaks at 17.78° and 34.21° are attributed to the $Ca(OH)_2$ phase whereas the peak at 32.92°, 39.82°, 53.31° and 65.12° were ascribed the characteristics of the CaO phase in the catalysts [23,38]. Comparable investigation results were also reported for animal bone [19], chicken bone [52], ostrich bone [20] and bovine teeth [48]. According to the XRD analysis, the principal components contained in the calcined catalyst were CaO, $Ca_{10}(PO_4)_6OH_2$, $Ca(OH)_2$ and $Ca_3(PO_4)_2$. X–ray diffraction analysis of catalyst (mixture of 25wt% teeth and 75wt% bone) obtained hexagonally packed crystal belonging to P63/m space group where the directional induce must be converted to Miller–Bravais point the induce in Miller–Bravais scheme which had hexagonal analysis scheme. The intensity at 2θ of 32.03° (112) and 33.23° (300) of calcined sample confirms the pure 100% crystalline HAp occurred in mixture of teeth and bone [24]. Thus, the change in the ratio of the intensity between the (112) and (300) peaks to the intensity of (300) diffraction peak of HAp is a strong indication of the change in the degree of crystallinity from 68.35% to 96.2% up on calcination [24]. A similar investigation by Figueiredo et al [40] was reported 80%, 94% and 95% crictallinity for calcined bovine bone at 600 °C, 900 °C and 1200 °C, respectively. Further the inorganic composition of mixture of 25wt% teeth and 75wt% bone before and after calcination in the form of oxides was analyzed by XRF and presented in Table 4.

The XRF analysis shows that more than 95% the oxides present in both calcined and uncalcined samples were for CaO and P_2O_5. Similar results were observed for calcined animal bone [20], cow bone [21] and bovine bone [53]. However, the mixture of 25wt% teeth and 75wt% bone for the present sample consist of other metal oxides such as MgO, Na_2O, Al_2O_3, Fe_2O_3 in lesser amount. Hence, the presence of the mentioned metal oxides enhance the catalytic activity for the transesterification reaction [20].

3.5. Physio-chemical properties of produced CO FAME

The physico-chemical properties of the produced CO FAME were analyzed by ASTM standard and the obtained results are shown in Table 5. The result shows that most of the physico-chemical properties were found to be within the limit of the standard of biodiesel. The acid value, density, viscosity, heating value of fatty acid methyl esters depend on the fatty acid composition of oil and variation occurred due to the degree of saturation and unsaturation in the alkyl group of fatty acids of vegetable oil. The acid value, specific gravity and kinematic viscosity of the produced CO FAME were found to be 0.41 mg KOH/g, 0.908 and 13.52 mm^2/s, respectively. The results were slightly lower than other origin of castor seed oil FAME [54]. The lower value kinematic viscosity (13.52 mm^2/s) of CO FAME produced by transesterification indicated that the conversion of the triglyceride to methyl ester. The amount of energy released per mass of produced CO FAME was 40.46 MJ/kg which was comparable with petroleum diesel and meet ASTM standard (Table 5). Cold flow property (i.e. cloud point) of the produced CO FAME was 3 °C. The result of cloud point makes CO FAME (biodiesel) appropriate for engine operation in moderate cold weather conditions. The total amount of unsaturated fatty acid or double bond present in produced FAME was indicated the quantity of double bond present on it which satisfies the ASTM requirement of a maximum of 115 and the presence of a double bond or higher amount of unsaturation in the carbon chain and CH_2–allylic position provides the oxidation reaction better. The dimensionless speed of combustion or auto-ignition from the

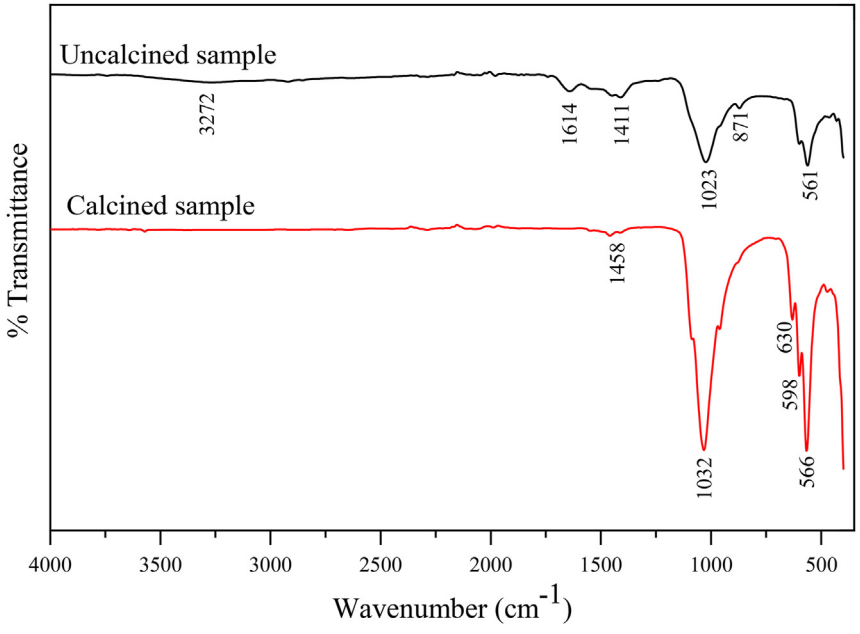

Figure 7. FT-IR spectra of mixture of waste animal teeth (25wt%) and bone (75wt%) before calcination and after calcination 1150 °C.

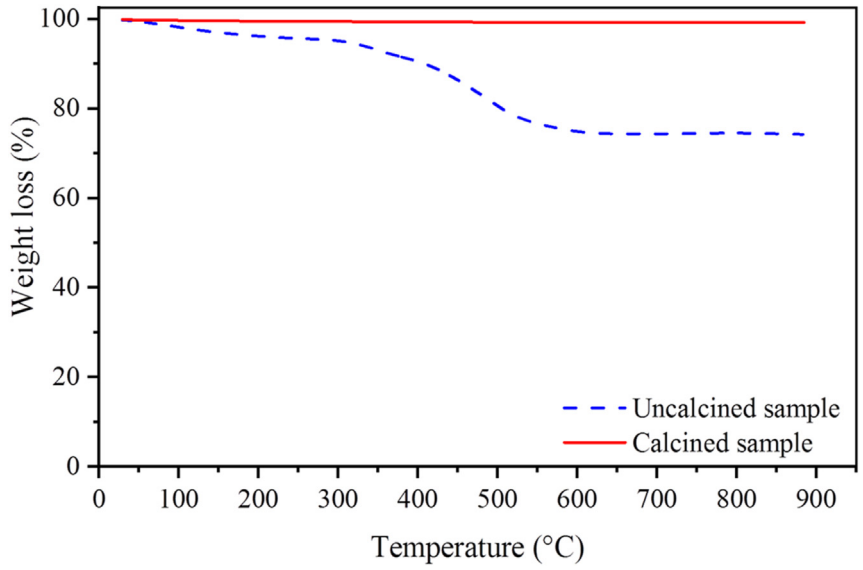

Figure 8. TG profile of mixture of 25wt% teeth and 75wt% bone without calcination and calcined at 1150 °C.

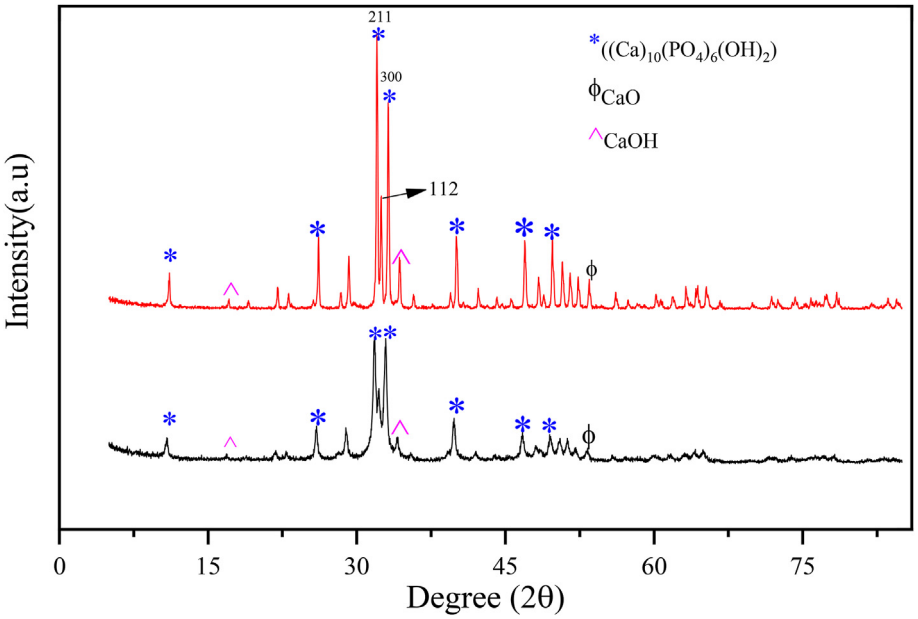

Figure 9. XRD pattern of mixture of waste animal teeth (25wt%) and bone (75wt%) before calcination (uncalcined) and after calcination at 1150 °C (calcined).

beginning of injection to engine of biodiesel was determined through an indirect method of cetane number proposed by Piyaporn et al. [55] (eq. 5). The estimated cetane number was 74.65 which indicates the high amount of oxygen present and good auto-ignition property and it was comparable to biodiesel obtained from coconut oil (70) [29].

$$CN = 46.3 + \frac{54.58}{SV} - 0.225IV \quad (5)$$

Where CN is cetane number, SV is saponification value and IV is iodine value.

3.6. Compositional analysis of produced CO FAME

The FT-IR spectra of CO and its FAME are presented in Figure 10. The spectra the samples was observed similar with slight peak shifting between CO and produced CO FAME; where the peak appeared at 3380, 2923, 1741, 1459, 1370, 1238, 1161 and 722 was shifted to 3431, 2924, 1738, 1438, 1360, 1244, 1171 and 723cm^{-1}, respectively. From 300–3500cm^{-1}, 2920–2930cm^{-1}, 2850–2855cm^{-1}, 1728–1750cm^{-1}, 1320–1370cm^{-1} and 1235–1245 cm^{-1} from indicated that the existence of –OH stretching of hydroxyl ricinoleic fatty acid alkyl group, CH_2 asymmetric stretching, CH_2 symmetric stretching, C=O stretching or carbonyl and ester, C=O symmetric stretching or deprotonated carboxyl and C–N stretching, respectively [19,42]. The peak obtained at 721 cm^{-1} confirmed the rocking vibration of $(–CH_2)_n$ overlapping [19]. In addition to peak shifting the carbonyl groups (–C=O) and (–C–O)' –OH group present in the structure of the esters, are naturally involved in reactions [56,57]. A similar result was also reported for castor seed oil-based FAME (biodiesel) [57]. Further, the qualitative results were confirmed by GC–MS (Figure 11), ^{1}H NMR (Figure 12) and ^{13}C NMR (Figure 13).

Based on the GC-MS analysis the produced CO FAME was consists of various fatty acid methyl esters such as ricinoleic FAME (83.74%), linoleic FAME (6.198%), oleic FAME (5.99%), stearic FAME (2.16%) and

Table 4. XRF analysis of mixing ratio of 25wt% animal teeth and 75wt% animal bone with and without calcined.

Oxides	Present study (wt%)		Calcined Animal Bone (wt%) [4]	Calcined Cow Bone (wt%) [30]	Bovine Bone (wt%) [32]
	Uncalcined	Calcined at 1150 °C			
CaO	54	61.32	66.4	64.89	52.25
P_2O_5	39.45	35.18	29.2	34.2	38.37
MgO	0.58	0.92	1.4	-	0.41
Na_2O	0.29	1.88	0.6	-	-
SO_3	0.08	0.39	0.5	-	-
Al_2O_3	0.49	0.49	0.05	-	-
Fe_2O_3	0.27	0.27	0.04	0.22	-
CO_2	-	-	1.7	-	-
SiO_2	0.44	0.44	0.02	-	-
ZnO	0.02	0.02	0.02	0.022	-

Table 5. Comparison of the physico-chemical properties of produced CO FAME with literature results.

Properties	Test Methods	Standard ASTM D6751-03		Present study (CO FAME)	Reference [51]
		FAME	Diesel		
Acid value	ASTM D 664	0.8 max	0.35	0.410 ± 0.024	0.875
Saponification value	AOCS Cd 3b-76	–	–	204.57 ± 1.053	–
Moisture content	–	0.05 max	0.05 max	0.05 ± 0.001	–
Specific gravity	ASTM D 4052	0.875–0.9	–	0.909 ± 0.035	0.916
Calorific value (MJ/Kg)	ASTM D240	35min	45.62–46.48	40.46 ± 1.027	–
Kinematic viscosity at 40 °C (mm^2/s)	ASTM D 445	1.5–6.0	–	13.52 ± 0.201	15.8
Flash point (°C)	ASTM D 93	130min	52–96	135 ± 2	–
Cetane number	ASTM D 613	47min	40min	74.65 ± 1.05	–
Cloud point (°C)	ASTM D6751	(-3)–12	(-15)–5	3 ± 0.367	–
Iodine value (gI2/100g)	AOCS official method 993.20	120max	–	112 ± 0.118	–

palmitic FAME (1.91%) (Table 6). The fatty acid profile of produced CO FAME is high in ricinoleic FAME content. Similar observation was also reported for different origin castor seed oil fatty acid methyl esters with higher ricinoleic FAME (89.27–90.87%) as compared to linoleic (4.21–5.0%), oleic (2.57–3.53%), stearic (0.13–1.1%) and palmitic (0.41–1.01%) FAME [58,59,60]. The slight difference in the composition of each fatty acid alkyl group was attributed to genotype of the original feedstock (castor seed).

Further, the confirmation of the conversion of the triglyceride to FAME and structure of the produced FAME was analyzed by ^{1}H NMR and ^{13}C NMR (Figures 12 and 13). ^{1}H NMR spectrum at 3.61 ppm demonstrates the –CH_3 of the methyl group present in the sample. The result was also confirmed by ^{13}C NMR analysis at around 51ppm. The peak at around 3.5ppm and 71ppm in ^{1}H NMR and ^{13}C NMR, respectively was correspond to –CH–OH due to presence of riciloneic fatty acid alkyl group. Similarly, the unsaturation due to presence of riciloneic, linoleic and oleic fatty acid alkyl group was observed at peak within range of 1120–135ppm in ^{13}C NMR. Further, the carbonyl (–C=O–) castor seed oil fatty acid methyl esters was clear appeared at around 174ppm (Figure 13). The chemical structure showed by GC-MS and NMR was

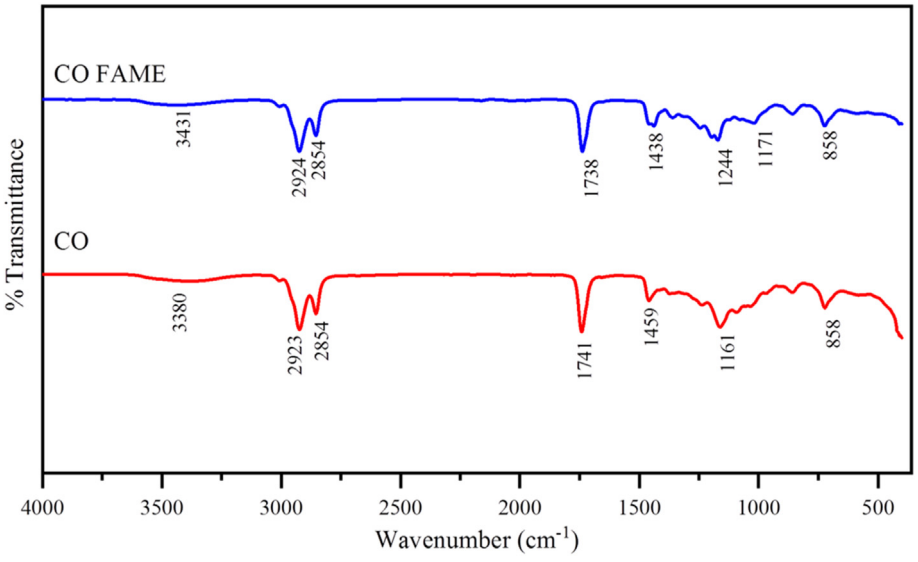

Figure 10. FT-IR spectra of castor oil (CO) and its fatty acid methyl ester (CO FAME) obtained using calcined catalyst from mixture of 25wt% teeth and 75wt% bone calcination temperature of 1150 °C.

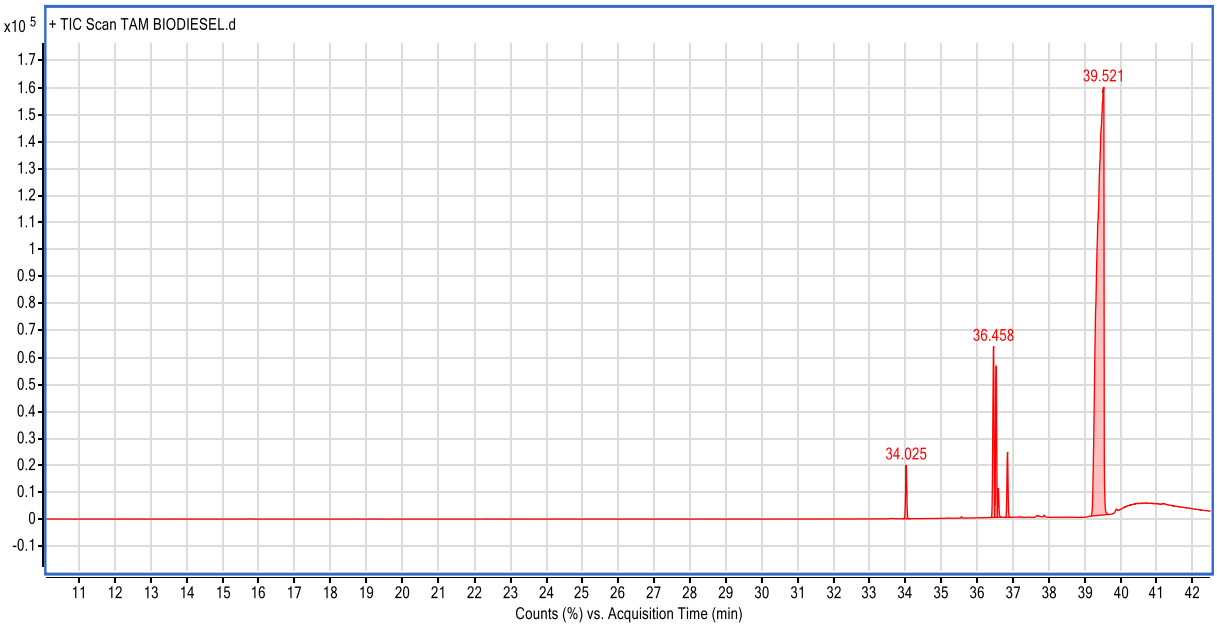

Figure 11. Gas chromatography-mass spectrometry (GC-MS) spectra of CO FAME.

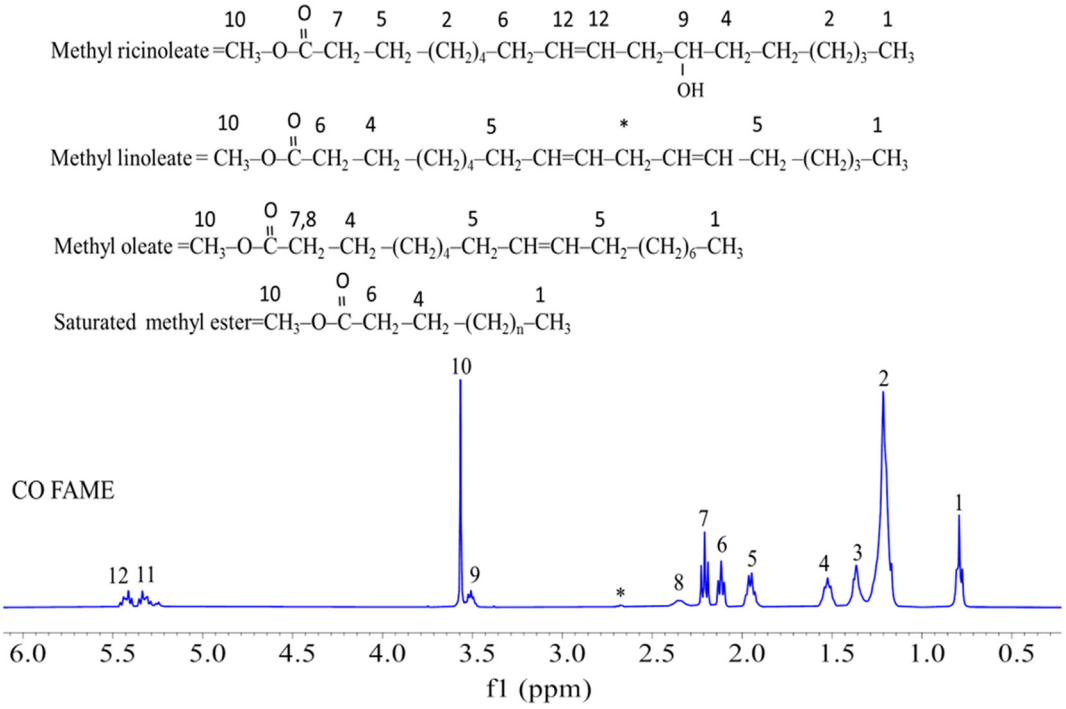

Figure 12. ^{1}H spectra for CO FAME obtained using calcined catalyst from mixture of 25wt% teeth and 75wt% bone calcination temperature of 1150 °C.

higher content of ricinoleic FAME with 92.6wt% conversion of CO triglycerides to CO FAME and purity of 92.6% of the produced CO FAME (eq. 4).

3.7. Flow behavior of produced CO FAM

The profile of shear stress and shear rate for the produced CO FAME at 25 °C is presented in Figure 14. The plot is linear relationship and passes through the origin with constant slope with R^2 value near to unit (1). The dynamic viscosity of CO FAME shows approximately a similar flow pattern within shear rate range of 50–300s^{-1}. Additionally, flow behavior of CO FAME were analyzed using power law model to estimate flow consistency (k) and non-Newtonian flow behavior indexes (n) at 25 °C from the linearization of power law equation (eq. 6) [61,62]. Generally, for shear thinning behavior corresponds to n less than unity (1), shear thickening behavior to n greater than unity (1) and Newtonian behavior to n equal to unity (1) [61,62]. Non-Newtonian flow behavior index (n) and flow consistency index or viscosity (k) for CO FAME at 25 °C was found to be 0.997 ± 0.0094 and 24.62 mpa, respectively. The result of Newtonian flow behavior index (n) indicated as the produced CO FAME was Newtonian fluid in nature within shear rate range from 50 to 300s^{-1}. Similar observation was reported for castor seed oil-based fatty acid methyl ester obtained by homogeneous catalysis [62].

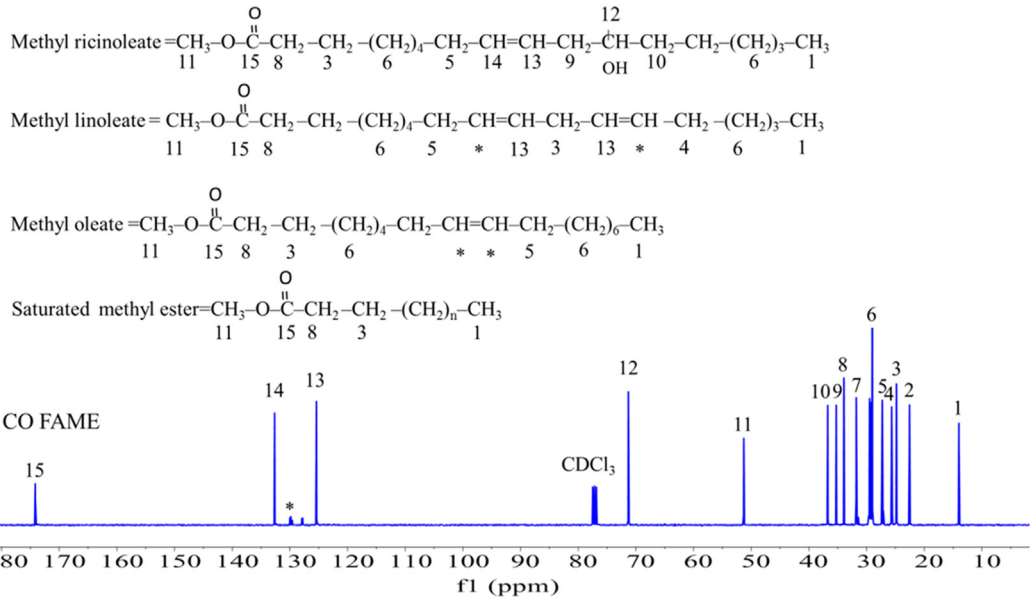

Figure 13. ^{13}C NMR spectra for CO FAME obtained using calcined catalyst from mixture of 25wt% teeth and 75wt% bone calcination temperature of 1150 °C.

Table 6. Comparison of major components of the produced CO FAME identified by GC-MS with the previous reported data.

Ester Composition	Present study			Other study		
	Acquisition time (min)	Amount (%)	Probability (%)	[14]	[36]	[35]
Ricinoleic FAME	39.5	83.74	94.3	89.27	90.87	89.15
Stearic FAME	36.85	2.16	83.25	0.16	0.13	1.1
Oleic FAME	36.53	5.99	82.46	3.53	2.57	3.3
Linoleic FAME	36.46	6.198	86.23	4.21	5.00	4.61
Palmitic FAME	34.03	1.91	87.5	0.92	0.41	1.01

$$ln(\tau) = ln(k) + nln(\gamma) \quad (6)$$

Where: τ, γ, n and k are shear stress (Pa), shear rate (s^{-1}), power-law coefficients and flow consistency index (Pa.s^n), respectively.

Furthermore, the viscosity of CO FAME was reduced non-linearly as the temperature increased from 25 °C to 80 °C (Figure 15). The result shows the dynamic viscosity of the produced FAME reduce from 22.5 to 3.32 mpa. s this indicated as the fluid flow resistance diminishes as the temperature rises due to molecular free movement.

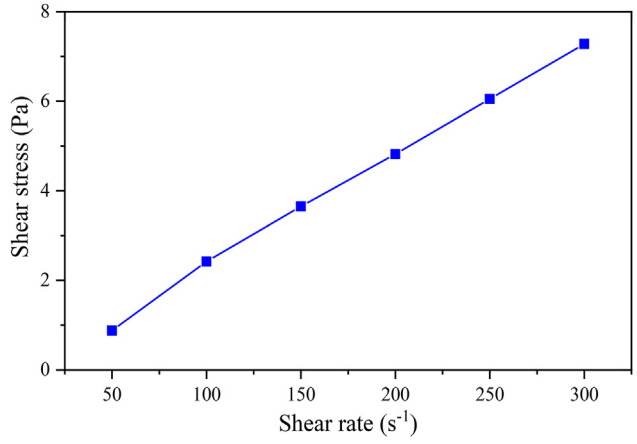

Figure 14. Relationship between shear stress and a shear rate of produced CO FAME at 25 °C.

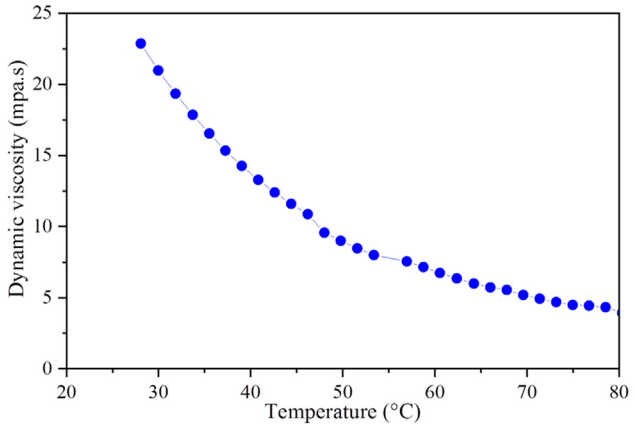

Figure 15. Effect of temperature on the dynamic viscosity produced CO FAME.

4. Conclusion

In the present study, various mixture of waste animal (0–100wt%) teeth and (0–100wt%) bone was utilized as raw materials for catalyst synthesis for the production of castor seed oil fatty acid methyl ester. Based on TGA of animal bone and teeth major component decomposition completed 650 °C for teeth and 550 °C for bone. Hence, the calcination temperature was fixed from 650 °C to 1250 °C with increments of 100 °C. Calcination temperature from 650–950 °C has significant effect on basicity of the catalyst produced from various mixture of animal bone and teeth. However, higher basicity value of 6.12mmol HCl/g was obtained at the calcination temperature of 1150 °C for mixing ratio of 25wt% teeth

and 75wt% bone with maximum yield of FAME (92.6wt%). The produced catalyst was composed of CaO (61.32wt%), P_2O_5 (35.18wt%) and other trace oxides as determined by XRF analysis. The catalyst obtained at the calcination temperature of 1150 °C for mixing ratio of 75wt% bone and 25wt% teeth was 96.2% crystalline. Further, the physico-chemical properties the produced CO FAME by using animal bone and teeth based catalyst was within the limit of the standard of biodiesel. Additionally, the produced CO FAME was Newtonian fluid in nature. Based on the current study finding, mixture of waste bone and teeth are found to be promising raw materials for catalyst synthesis for transesterification of castor seed oil with good reusability. Furthermore, parametric effect, optimization and cost analysis for larger scale production of biodiesel from any feedstocks using the produced catalyst are recommended for future research.

Declarations

Author contribution statement

Tamrat Getachew Mengistu: Conceived and designed the experiments; Performed the experiments; Analyzed and interpreted the data; Contributed reagents, materials, analysis tools or data; Wrote the paper.

Ali Shemsedin Reshad: Conceived and designed the experiments; Analyzed and interpreted the data; Wrote the paper.

Funding statement

This research did not receive any specific grant from funding agencies in the public, commercial, or not-for-profit sectors.

Data availability statement

The datasets generated during and/or analysed during the current study are available from the corresponding author on reasonable request.

Declaration of interests statement

The authors declare no conflict of interest.

Additional information

No additional information is available for this paper.

References

[1] H. Fukuda, A. Kond, H. Noda, Biodiesel fuel production by transesterification of oils, J. Biosci. Bioeng. 92 (2001) 405–416.
[2] J.V. Gerpen, Biodiesel processing and production, Fuel Process. Technol. 86 (2005) 1097–1107.
[3] A.P. Vyas, J.L. Verma, N. Subrahmanyam, A review on FAME production processes, Fuel 89 (2010) 1–9.
[4] Z. Helwani, M.R. Othman, N. Aziz, W.J.N. Fernando, J. Kim, Technologies for production of biodiesel focusing on green catalytic techniques: a review, Fuel Process. Technol. 90 (2009) 1502–1514.
[5] T. Issariyakul, A.K. Dalai, Biodiesel from vegetable oils, Renew. Sustain. Energy Rev. 31 (2014) 446–471.
[6] D.S. Ogunniyi, Castor oil: a vital industrial raw material, Bioresour. Technol. 97 (2006) 1086–1091.
[7] V. Scholza, J.N. da Silva, Prospects and risks of the use of castor oil as a fuel, Biomass Bioenergy 32 (2008) 95–100.
[8] L. Lin, Z. Cunshan, S. Vittayapadung, S. Xiangqian, D. Mingdong, Opportunities and challenges for biodiesel fuel, Appl. Energy 88 (2011) 1020–1031.
[9] G. Vicente, M. Martinez, J. Aracil, Integrated biodiesel production: a comparison of different homogeneous catalysts systems, Bioresour. Technol. 92 (2004) 297–305.
[10] U. Jamil, A.H. Khoja, R. Liaquat, S.R. Naqvi, W.N.N.W. Omar, N.A.S. Amin, Copper and calcium-based metal organic framework (MOF) catalyst for biodiesel production from waste cooking oil: a process optimization study, Energy Convers. Manag. 215 (2020) 1–14.
[11] A.E. Atabani, A.S. Silitonga, I.A. Badruddin, T.M.I. Mahlia, H.H. Masjuki, S. Mekhilef, A comprehensive review on biodiesel as an alternative energy resource and its characteristics, Renew. Sustain. Energy Rev. 16 (2012) 2070–2093.
[12] S.T. Tolera, F.K. Alemu, Potential of abattoir waste for bioenergy as sustainable management, eastern Ethiopia, 2019, J. Energy 2020 (2020) 1–9.
[13] F. Hussain, S. Alshahrani, M.M. Abbas, H.M. Khan, A. Jamil, H. Yaqoob, et al., Waste animal bones as catalysts for biodiesel production; a mini review, Catalysts 11 (2021) 1–15.
[14] N. Regassa, R.D. Sundaraa, B.B. Seboka, Challenges and opportunities in municipal solid waste management: the case of addis ababa city, central Ethiopia, J. Hum. Ecol. 33 (2017) 179–190.
[15] K. Buddhachat, S. Klinhom, P. Siengdee, J.L. Brown, R. Nomsiri, P. Kaewmong, et al., Elemental analysis of bone, teeth, horn and antler in different animal species using non-invasive handheld X-ray fluorescence, PLoS One 11 (2016) 1–21.
[16] A. Obadiah, G.A. Swaroopa, S.V. Kumar, K.R. Jeganathan, A. Ramasubbu, Biodiesel production from palm oil using calcined waste animal bone as catalyst, Bioresour. Technol. 116 (2012) 512–516.
[17] S. Ramesh, Z.Z. Loo, C.Y. Tan, W.J.K. Chew, Y.C. Ching, F. Tarlochan, et al., Characterization of biogenic hydroxyapatite derived from animal bones for biomedical applications, Ceram. Int. 44 (2018) 10525–10530.
[18] S.M. Smith, C. Oopathum, V. Weeramongkhonlert, C.B. Smith, S. Chaveanghong, P. Ketwong, et al., Transesterification of soybean oil using bovine bone waste as new catalyst, Bioresour. Technol. 143 (2013) 686–690.
[19] J. Nisar, R. Razaq, M. Farooq, M. Iqbal, R.A. Khan, M. Sayed, et al., Enhanced biodiesel production from Jatropha oil using calcined waste animal bones as catalyst, Renew. Energy 101 (2017) 111–119.
[20] H.M. Khan, T. Iqbal, C.H. Ali, A. Javaid, I.I. Cheema, Sustainable biodiesel production from waste cooking oil utilizing waste ostrich (*Struthio camelus*) bones derived heterogeneous catalyst, Fuel 277 (2020) 1–10.
[21] A.A. Ayodeji, I.E. Blessing, F.O. Sunday, Data on calcium oxide and cow bone catalysts used for soybean biodiesel production, Data Brief 18 (2018) 512–517.
[22] R. Chakraborty, S. Bepari, A. Banerjee, Application of calcined waste fish (*Labeo rohita*) scale as low-cost heterogeneous catalyst for biodiesel synthesis, Bioresour. Technol. 102 (2011) 3610–3618.
[23] M. Farooq, A. Ramli, A. Naeem, Biodiesel production from low FFA waste cooking oil using heterogeneous catalyst derived from chicken bones, Renew. Energy 76 (2015) 362–368.
[24] G.M. Jr Poralan, J.E. Gambe, E.M. Alcantara, R.M. Vequizo, X-ray diffraction and infrared spectroscopy analyses on the crystallinity of engineered biological hydroxyapatite for medical application, in: 1st International Conference in Applied Physics and Materials Science 79, 2015, pp. 1–6.
[25] H.G. Karge, Handbook of heterogeneous catalysis, in: Acidity and Basicity Concepts and Anlysis, Wiley Online Library, 2008.
[26] T. Kozo, M. Makoto, O. Yoshio, H. Hideshi, Determination of acidic and basic properties on solid surfaces, in: New Solid Acids and Bases - Their Catalytic Properties, 1989, pp. 5–25.
[27] A.K. Singh, S.D. Fernando, Transesterification of soybean oil using heterogeneous catalysts, Energy Fuel. 22 (2008) 2067–2069.
[28] V. Volli, M.K. Purkait, C.-M. Shu, Preparation and characterization of animal bone powder impregnated fly ash catalyst for transesterification, Sci. Total Environ. 669 (2019) 314–321.
[29] A.J. Folayan, P.A.L. Anawe, Synthesis and characterization of Argania spinosa (Argan oil) biodiesel by sodium hydroxide catalyzed transesterification reaction as alternative for petro-diesel in direct injection, compression ignition engines, Heliyon 5 (2019), e02427.
[30] K.B. Hundie, D.A. Akuma, Optimization of biodiesel production parameters from *Prosopis julifera* seed using definitive screening design, Heliyon 8 (2022), e08965.
[31] S. Kumar, S. Jain, H. Kumar, Experimental study on biodiesel production parameter optimization of jatropha–algae oil mixtures and performance and emission analysis of a diesel engine coupled with a generator fueled with diesel/biodiesel blends, ACS Omega 5 (2020) 17033–17041.
[32] P. Purwanto, L. Buchori, I. Istadi, Reaction rate law model and reaction mechanism covering effect of plasma role on the transesterification of triglyceride and methanol to biodiesel over a continuous flow hybrid catalytic-plasma reactor, Heliyon 6 (2020), e05164.
[33] P. Schinas, G. Karavalakis, C. Davaris, G. Anastopoulos, D. Karonis, F. Zannikos, et al., Pumpkin (*Cucurbita pepo L.*) seed oil as an alternative feedstock for the production of biodiesel in Greece, Biomass Bioenergy 33 (2009) 44–49.
[34] M. Farooq, A. Ramli, D. Subbarao, Biodiesel production from waste cooking oil using bifunctional heterogeneous solid catalysts, J. Clean. Prod. 59 (2013) 131–140.
[35] A.S. Reshad, D. Panjiara, P. Tiwari, V.V. Goud, Two-step process for production of methyl ester from rubber seed oil using barium hydroxide octahydrate catalyst: process optimization, J. Clean. Prod. 142 (2017) 3490–3499.
[36] D.M.E. Santo Filho, F.L.B. de Abreu, R.G. Pereira, J.R.R. Siqueira, J.J.P. dos Santos Junior, R.J. Daroda, Characterization of density of biodiesel from soybean, sunflower, canola, and beef tallow in relation to temperature, using a digital density meter with a metrological point of view, J. ASTM Int. (JAI) 7 (2010) 1–6.
[37] A. Subcommittee, Standard Test Method for Kinematic Viscosity of Transparent and Opaque Liquids:(and Calculation of Dynamic Viscosity), ASTM International, 2006.
[38] Y.H. Tan, M.O. Abdullah, J. Kansedo, N.M. Mubarak, Y.S. Chan, C. Nolasco-Hipolito, Biodiesel production from used cooking oil using green solid catalyst derived from calcined fusion waste chicken and fish bones, Renew. Energy 139 (2019) 696–706.
[39] C.F. Ramirez-Gutierrez, S.M. Londoño-Restrepo, A. del Real, M.A. Mondragón, M.E. Rodriguez-García, Effect of the temperature and sintering time on the thermal, structural, morphological, and vibrational properties of hydroxyapatite derived from pig bone, Ceram. Int. 43 (2017) 7552–7559.

[40] M. Figueiredo, A. Fernando, G. Martins, J. Freitas, F. Judas, H. Figueiredo, Effect of the calcination temperature on the composition and microstructure of hydroxyapatite derived from human and animal bone, Ceram. Int. 36 (2010) 2383–2393.
[41] N.A.M. Barakat, M.S. Khil, A.M. Omran, F.A. Sheikh, H.Y. Kim, Extraction of pure natural hydroxyapatite from the bovine bones bio waste by three different methods, J. Mater. Process. Technol. 209 (2009) 3408–3415.
[42] T. Petit, L. Puskar, FTIR spectroscopy of nanodiamonds: methods and interpretation, Diam. Relat. Mater. 89 (2018) 52–66.
[43] J. Gupta, M. Agarwa, A.K. Dalai, Marble slurry derived hydroxyapatite as heterogeneous catalyst for biodiesel production from soybean oil, Can. J. Chem. Eng. 96 (2018) 1873–1880.
[44] P.V. Campos, A.R.L. Albuquerque, R.S. Angélica, S.P.A. Paz, FTIR spectral signatures of amazon inorganic phosphates: igneous, weathering, and biogenetic origin, Spectrochim. Acta Mol. Biomol. Spectrosc. 251 (2021) 1–12.
[45] Y. Liu, W. Wang, Y. Zhan, C. Zheng, G. Wang, A simple route to hydroxyapatite nanofibers, Mater. Lett. 56 (2002) 496–501.
[46] A. Sobczak-Kupiec, E. Olender, D. Malina, B.z. Tyliszczak, Effect of calcination parameters on behavior of bone hydroxyapatite in artificial saliva and its biosafety, Mater. Chem. Phys. 206 (2018) 158–165.
[47] J. Venkatesan, Z.J. Qian, B. Ryu, N.V. Thomas, S.K. Kim, A comparative study of thermal calcination and an alkaline hydrolysis method in the isolation of hydroxyapatite from Thunnus obesus bone, Biomed. Mater. 6 (2011) 1–12.
[48] A. Elkayar, Y. Elshazly, M. Assaad, Properties of hydroxyapatite from bovine teeth, L A 2 (2009) 31–36.
[49] I. Istadi, L. Buchori, B.B.T. Putri, H.I.A. Hantara, Effect of catalyst pellet-diameter and basicity on transesterification of soybean oil into biodiesel using K_2O/CaO-ZnO catalyst over hybrid catalytic-plasma reactor, in: MATEC Web of Conferences 156, 2018, pp. 1–4.
[50] N. Degirmenbasi, S. Coskun, N. Boz, D.M. Kalyon, Biodiesel synthesis from canola oil via heterogeneous catalysis using functionalized CaO nanoparticles, Fuel 153 (2015) 620–627.
[51] R. Rajesh, A. Hariharasubramanian, Y.D. Ravichandran, Chicken bone as a bioresource for the bioceramic (hydroxyapatite), Phosphorus, Sulfur Silicon Relat. Elem. 187 (2012) 914–925.
[52] S.-L. Bee, M. Mariatti, N. Ahmad, B.H. Yahaya, Z.A.A. Hamid, Effect of the calcination temperature on the properties of natural hydroxyapatite derived from chicken bone wastes, Mater. Today Proc. 16 (2019) 1876–1885.
[53] K. Haberko, M.M. Bućko, J. Brzezińska-Miecznik, M. Haberko, W. Mozgawa, T. Panz, et al., Natural hydroxyapatite—its behaviour during heat treatment, J. Eur. Ceram. Soc. 26 (2006) 537–542.
[54] J.M. Encinar, S. Nogales-Delgado, Nuria Sánchez, J.F. González, Biolubricants from rapeseed and Castor oil transesterification by using titanium isopropoxide as a catalyst: production and characterization, Catalysts 10 (2020) 1–12.
[55] P. Kalayasiri, N. Jeyashoke, K. Krisnangkura, Survey of seed oils for use as diesel fuels, JAOCS (J. Am. Oil Chem. Soc.) 73 (1996) 471–474.
[56] L.F.B. de Lira, M.S. de Albuquerque, J.G.A. Pacheco, T.M. Fonseca, E.H.d.S. Cavalcanti, L. Stragevitch, et al., Infrared spectroscopy and multivariate calibration to monitor stability quality parameters of biodiesel, Microchem. J. 96 (2010) 126–131.
[57] R.K. Elango, K. Sathiasivan, C. Muthukumaran, V. Thangavelu, M. Rajesh, K. Tamilarasan, Transesterification of castor oil for biodiesel production: process optimization and characterization, Microchem. J. 145 (2019) 1162–1168.
[58] P. Berman, S. Nizri, Z. Wiesman, Castor oil biodiesel and its blends as alternative fuel, Biomass Bioenergy 35 (2011) 2861–2866.
[59] S.T. Keera, S.M.E. Sabagh, A.R. Taman, Castor oil biodiesel production and optimization, Egypt J. Pet. 27 (2018) 979–984.
[60] M. Kılıç, B.B. Uzun, E. Pütün, A.E. Pütün, Optimization of biodiesel production from castor oil using factorial design, Fuel Process. Technol. 111 (2013) 105–110.
[61] F.A. Holland, R. Bragg, Fluid Flow for Chemical Engineers, 1994.
[62] A.K. Paul, V.B. Borugadda, A.S. Reshad, M.S. Bhalerao, P. Tiwari, V.V. Goud, Comparative study of physicochemical and rheological property of waste cooking oil, castor oil, rubber seed oil, their methyl esters and blends with mineral diesel fuel, Mater. Sci. Energy Technol. 4 (2021) 148–155.